Tribology International 200 (2024) 110083

Contents lists available at ScienceDirect

Tribology International

journal homepage: www.elsevier.com/locate/triboint

Full Length Article

The influence of pin inclination on frictional behaviour in pin-on-disc sliding and its implications for test reliability

Hongzhi Yue [a,*], Johannes Schneider [a], Bettina Frohnapfel [b], Peter Gumbsch [a]

[a] Institute for Applied Materials - Reliability and Microstructure (IAM-ZM) and MicroTribology Center μTC, Karlsruhe Institute of Technology (KIT), Karlsruhe, 76131, Germany

[b] Institute of Fluid Mechanics (ISTM), Karlsruhe Institute of Technology (KIT), Karlsruhe, 76131, Germany

ARTICLE INFO

Keywords:
Pin-on-disc test
Pin inclination
Mixed or hydrodynamic lubrication
Multi-scale modelling

ABSTRACT

The pin-on-disc test is a widely employed method for investigating the friction and wear performance of materials in conformal contact. In a typical pin-on-disc system, self-aligning pin holders are frequently utilized to ensure proper surface contact. This study reveals that in such a setup, pin inclination has a significant impact on test reliability, particularly under oil-lubricated conditions, which may overweight the influence of other parameters such as roughness or texture elements. Utilizing in-situ measurements, we captured the dynamic changes in pin inclination during rotational sliding. Our findings indicate that the pin inclination varies with sliding speed, showing a pitch angle difference of approximately 0.01° as the speed decreases from 2 m/s to 0.04 m/s in our test setup. Importantly, a robust correlation was identified between the friction coefficient and pin inclination, which is supported by the numerical investigation. This study underscores concerns regarding the test reliability of pin-on-disc tribometers, prompting a reconsideration of the assumptions associated with self-aligning pin holders in such experimental configurations.

1. Introduction

In order to meet stricter economic and ecological requirements, tribological systems are often expected to have low friction, minimal wear and high mechanical resistance. In many of the engineering applications, friction arises within conformal contact scenarios, including sliding guides [1,2], braking system [3,4], mechanical sealing [5,6] or artificial joint [7]. Conformal contact refers to a situation in which two surfaces or objects come into contact with each other in a way that their surface geometries match or conform to each other precisely [8]. In sliding friction applications, achieving conformal contact is often desirable to lower pressure, minimize wear, reduce friction, and enhance the overall efficiency and performance of mechanical systems.

Pin-on-disc test is a standard test method to test the friction and wear performance on materials in conformal contact [9,10]. In a typical system, a fixed pin is exerted onto a disc in rotational motion by a given load. In most cases, self-aligning pin holders are used to ensure flat-on-flat contact [11–13]. The setup is expected to overcome the minor slopes on the disc surface due to misalignment or surface waviness and provide stationary friction. With the given setups, the friction force is expected to be stationary. However, in practice, periodic friction fluctuation is always inevitable [14–16]. Friction oscillations are commonly associated with anisotropic roughness, system oscillation, or the periodic motion of the pin in the loading direction caused by the height waviness of the contacting surface [17]. Nonetheless, distinct pin inclination states may also arise due to force fluctuations, potentially amplifying the impact of the above mentioned disturbance. According to hydrodynamic lubrication theory, the pitch angle between rubbing surfaces plays a pivotal role in generating hydrodynamic lift. Only a convergent gap between sliding surfaces could generate positive hydrodynamic pressure and result in a lifting force [18]. Research on tilting pad bearings [19,20] demonstrates how pin inclinations are generated in pivot support structures, consequently influencing friction. Similar conditions were observed for the self-aligning pin; however, the existence of pin inclination during sliding and its effects are frequently overlooked.

In this study, we performed in-situ measurements to illustrate the dynamic variation of pin inclination during sliding in a self-aligning pin-on-disc test. The correlation between friction and pin inclination was analysed. A numerical study was carried out to explain the impact of this observed behaviour.

* Corresponding author.
E-mail addresses: hongzhi.yue@kit.edu (H. Yue), johannes.schneider@kit.edu (J. Schneider), bettina.frohnapfel@kit.edu (B. Frohnapfel), peter.gumbsch@kit.edu (P. Gumbsch).

https://doi.org/10.1016/j.triboint.2024.110083
Received 18 June 2024; Received in revised form 5 August 2024; Accepted 6 August 2024
Available online 8 August 2024

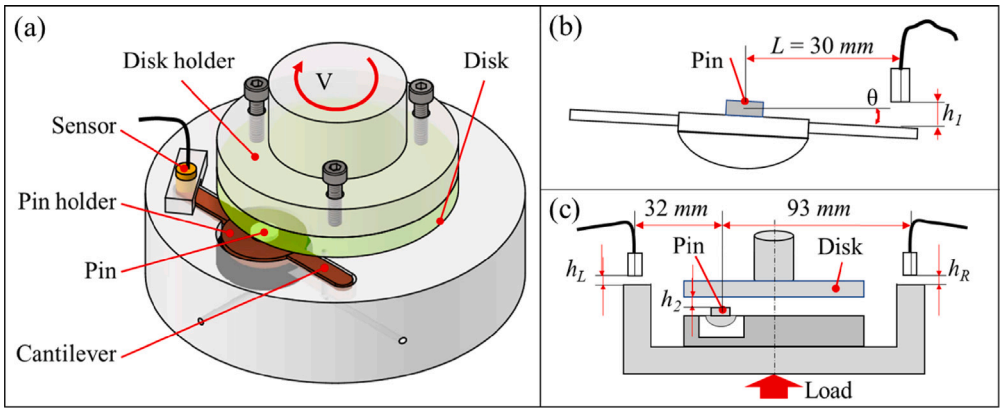

Fig. 1. Schematic representation of (a) the pin-on-disc tribometer, (b) the inclination measurement setup and (c) gap height measurement setup.

2. Methods

2.1. Experiments

The rotational experiments were conducted in a tribometer (Plint TE-92 HS, Phoenix Tribology, Kingsclere, UK) using a pin-on-disc set-up. The cylinder pins of 8 mm diameter made from 100Cr6 with an average hardness of 713 HV were purchased from SKF (SKF, Fothenburg, Sweden). The 70 mm diameter discs made out of 100Cr6 with an average hardness of 800 HV were lapped to reach an isotropic roughness pattern. The averaged sample roughness before the tests was $Ra = 0.2$ μm for the pin and $Ra = 0.07$ μm for the disc, as measured by a stylus profilometer (Hommel T8000, Jenoptic, Jena, Germany).

As shown in Fig. 1a, the pin was fixed on a self-aligned holder, while the disc sample was mounted on the rotating spindle. Three screws on the back of the disc were used to minimize the misalignment or other mounting errors of the disc. The tribometer set-up was modified to monitor the in-situ variation of inclination. The pin holder was extended through a rigid cantilever that allows the pitch angle to be measured, with the distance between the centre of the pin and the sensor $L = 30$ mm. A fixed proximity sensor (AW 210-22-1, E+H Metrology, Karlsruhe, Germany) was used to measure the distance to the end of the cantilever (h_1 in Fig. 1b). The pin inclination was characterized by the pitch angle $\theta = \arctan\frac{\Delta h_1}{L}$ according to the height variance Δh_1 and the distance L. The height at 0.25 m/s served as zero reference. The sensitivity of the sensor is less than 1 μm, leading to a measuring accuracy of less than 0.002° for the pitch angle. Furthermore, two more sensors were used to measure the distances h_L and h_R at both side of the lower parts with the distance to the pin centre of 33 mm and 93 mm, respectively. The gap height ($\Delta h_2 = 0.74\Delta h_L + 0.26\Delta h_R$ in Fig. 1c) was calculated based on the height variance Δh_L and Δh_R, with the lowest value as the zero reference.

During the tests, a normal load of 150 N was applied from the pin side. The disc started rotation from 2 m/s and gradually decreased to 0.04 m/s in 12 steps for each speed ramp. Five ramp repetitions were conducted for the speed ramps and only the last three ramps were calculated to avoid the running-in effects. Each speed step last for 5 min for averaging friction using 10 Hz sampling rate. At the end of each speed step, the friction and height variation in three revolutions were recorded at high sampling rate triggered by the encoder of 2048 pulses per revolution (ppr). The coefficient of friction (CoF) was averaged from the results of 5 min data and 3 revolution high frequency data separately.

The experiments were conducted at oil temperature of 50 °C. An additive-free FVA 2 oil was used in the test. The oil viscosity value was 0.024 Pa s at 50 °C, measured by a rheometer (DHR series, TA instruments, New Castle, USA) at a shearing rate of ~500 s^{-1}. The oil was supplied to immerge the contact surface before the test start, and a constant oil flow rate was set at 5 ml/min during the whole test. The contact area was submerged in the oil during the whole test. The surface macro-topography was measured with the confocal microscope (FRT MicroProt 100, Fries Research & Technology GmbH, Bergisch Gladbach, Germany) with a size of 8 × 8 mm and the roughness profiles were measured with the white light interferometry profiler (Sensofar Plμ Neox, Sensofar Metrology, Barcelona, Spain) in a 256 μm × 192 μm square before and after the experiments. Flat pins were used for 5 repetitions in test 1, and a curved pin with very large radius (~0.9 m) was used for test 2 as a reference. The corresponding pin surface profiles in the tests are depicted in Fig. 2. Each individual repetition was conducted with new samples and fresh oil in the system.

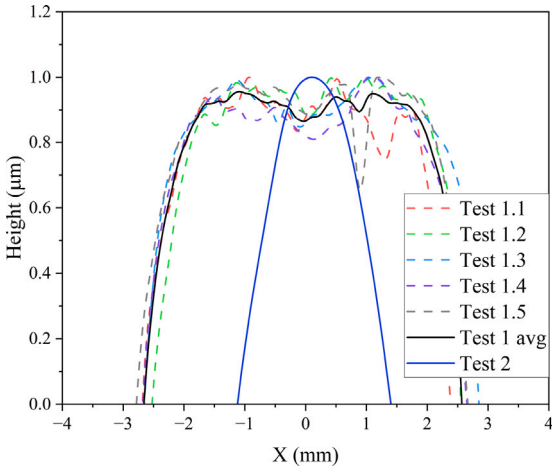

Fig. 2. Centre line plot of the virtual macroscopic pin topographies. Test 1 avg means the average value of 5 repetitions in test 1.

2.2. Simulation

The Pin-on-disc test was modelled numerically in this study, employing the Homogenized Mixed Elasto-Hydrodynamic Lubrication Fischer–Burmeister–Newton–Schur (HMEHL-FBNS) solver implemented in MATLAB©, as previously described in our earlier work [21]. To initiate the simulation, the macroscopic geometry was reconstructed from the 8 × 8 mm measured FRT image, with subsequent levelling of the profile at an imposed normal load of 50 N to ensure precise surface alignment. The simulation was then executed with the levelled profile and a 150 N load. The homogenized Reynolds equation was discretized using the finite volume method (FVM), wherein the Poiseuille terms were discretized with a second-order central scheme and the Couette term

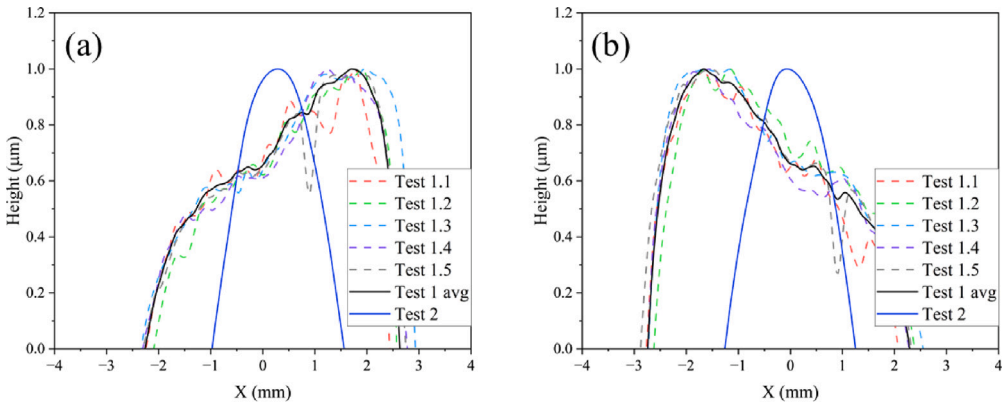

Fig. 3. Centre line plot of the virtual macroscopic pin topographies with (a) 0.01° and (b) −0.01° inclinations.

with a first-order upwind scheme. Consistently, the same roughness patch was applied for the homogenized method in all simulations.

Two distinct types of studies were simulated in this investigation. In the first study (Sim 1), simulations were executed using measured surface profiles devoid of any pre-set inclination, employing identical roughness patches as delineated in our preceding work [21]. In the second study (Sim 2), the model underwent an initial calibration with the experimental results of test 2, by scaling the roughness patch height to 0.65 of the original height while keeping the other parameters the same. Following calibration, pin surfaces with inclination were generated by tilting the surface profile within the range of −0.02 to 0.02° around the centre, as depicted in Fig. 3. Subsequently, the simulation results were acquired based on the prescribed test sliding speed and the measured pin inclination.

3. Results

3.1. Test results

Fig. 4 shows the optical and 3D microscopy images for different pins after experiments. The contact zone in test 1 is a circle with a diameter of around 5 mm for all tests (Fig. 4a and c). For test 2, the contact zone is much smaller due to the high curvature of the surface, resulting in a circular contact zone of 2.7 mm diameter. The surface roughness of the pins decreased due to sliding between the samples, reaching around Ra 0.07 μm for all the pins. No dramatic roughness differences were observed between different tests.

The Fig. 5a illustrates the variation in average Coefficient of Friction (CoF) of 3 revolutions with respect to sliding speed. As described in the experiment part, two methods were used to calculate the average CoF: the 5 min averaged low frequency data and the 3 revolution high frequency data. Only high speed results are shown here, as similar results were acquired for the two methods (Fig. S1 in the supporting information). Despite the surface macro profile and roughness being similar, significant disparities in frictional behaviours were observed among samples in test 1. Specifically, the CoF ranged from 0.059 for test 1.1 to 0.124 for test 1.4 at a sliding speed of 0.04 m/s. Notably, test 1.1, test 1.2, and test 1.5 exhibited lower friction, while test 1.3 and 1.4 demonstrated a seemingly "failed" state with disproportionately larger CoF. Furthermore, the transition speed from hydrodynamic lubrication to mixed lubrication varied across different tests, spanning from 0.1 to 0.25 m/s. Interestingly, despite substantial differences in pin surface profiles, test 2 displayed frictional behaviour similar to the low-friction samples in test 1. To decipher the causes behind the considerable frictional behaviour contrast observed in test 1, a comprehensive analysis was conducted on gap height and pin inclination during the tests. Fig. 5b depicts the variation in gap height with respect to sliding speed, with the minimum height serving as the zero reference. Surprisingly, elevated gap heights were observed for both high and low sliding speeds. This phenomenon arises from the combined effects of pin inclination and actual gap height. When the pin is parallel to the disc, the measured value represents the true gap height. Conversely, when an angle exists between the pin and disc, one side of the gap is elevated. Consequently, the reliability of the gap height data is compromised. Nonetheless, this discrepancy can be leveraged to establish the zero reference for the inclination. As the majority of the minimum values fall within the range of 0.15 to 0.4 m/s, the value at 0.25 m/s was chosen as the zero reference for the pitch angle. Fig. 5c depicts the variation in relative pitch angle with respect to sliding speed, with data at 0.25 m/s as the zero reference. With speed decreasing, the pitch angle also decreases, indicating diverging gap between the pin and the disc. The inclinations for the pins are relatively small with an angle around the scale of 0.01°. Minimum pitch angles range between −0.004° for test 2 to −0.018° for test 1.3 at 0.04 m/s. For the high friction tests (test 1.3 and test 1.4), a low pitch angle was also observed. The pitch angles at high sliding speed are more erratic, both positive and negative angle were observed. To further show the relation between friction and pin inclination, the average CoF was plotted with respect to the relative pitch angle as shown in Fig. 5d. A quasi-linear relation was observed between the friction and pin inclination for all tests.

To unravel the underlying reasons for the disparate friction behaviours, an in-depth analysis of friction variations within one rotating revolution was conducted. Data were meticulously recorded at a high sampling rate of 2048 times per revolution for three consecutive revolutions following each speed increment. Remarkably consistent results were observed for the high-speed data across different speed ramps, and data from the final speed ramp were specifically utilized in this investigation.

As illustrated in Fig. 6, the figure presents the characteristic variation of the CoF and relative pitch angle within one revolution against sliding speed for different tests. Low CoF values were consistently achieved throughout the entire revolution at high speed. As the sliding speed decreased, the friction coefficient exhibited an upward trend. In certain instances, the frictional behaviour exhibited high variation, characterized by the formation of three distinct peak fluctuations within one revolution. Conversely, in other cases, the friction demonstrated a more stable profile. Concurrently, the pitch angle displayed three peak fluctuations in all tests across the entire speed range. This pitch angle fluctuation is attributed to the disc being supported by three screws (at ~60, 180 and 300°) to facilitate alignment adjustments. Consequently, the measured inclination is a blend of the actual pitch angle and the inclination resulting from the intrinsic height variation of the disc. The pitch angle vibration remains relatively consistent at high speeds. However, as the speed decreases, not only does the average value of the pitch angle change, but the profile within one revolution also undergoes alterations.

Fig. 7a shows the CoF and relative pitch angle change within one revolution at 0.04 m/s for all tests. Apart from the high friction tests

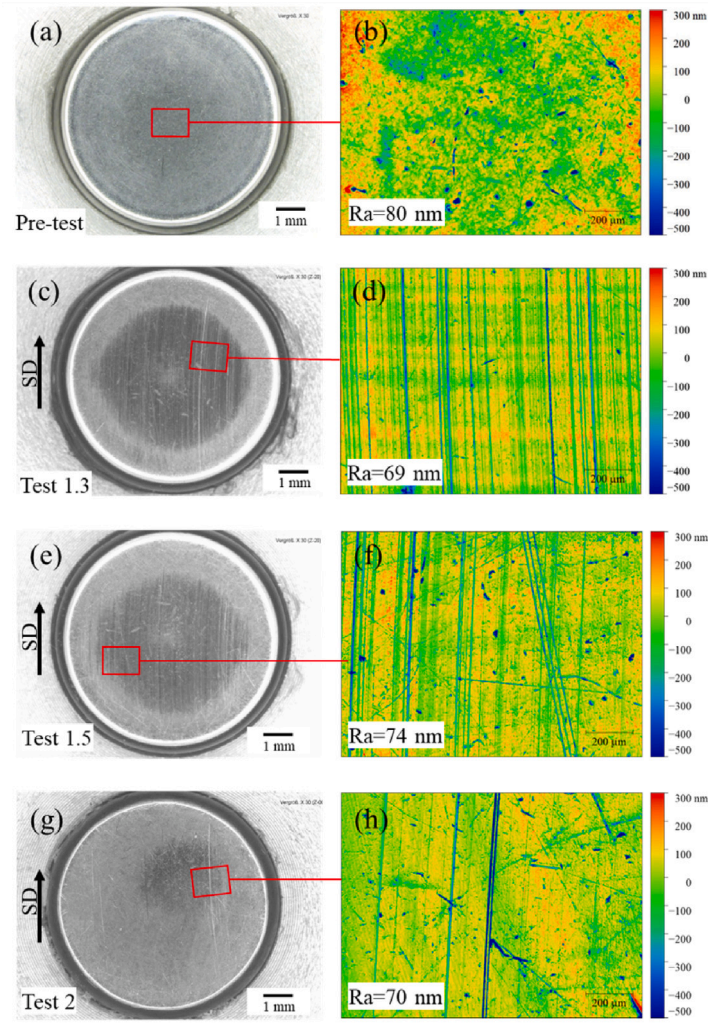

Fig. 4. Topographies of post-test pin surfaces. Black arrow marked SD denotes for the sliding direction.

(test 1.3 and test 1.4), the average frictions are close to each other with average CoF of ~0.06°. However, for some tests (test 1.1 and test 1.5) the friction is fluctuating in very wide range, while others (test 1.2 and test 2) are more stable. Fig. 7b illustrates the relative pitch angle over one revolution at 0.04 m/s, with the height h_1 at 0.25 m/s serving as the zero reference. The pin inclination also demonstrates distinct patterns in various tests. Both pitch angle and coefficient of friction exhibit analogous fluctuations. Tests 1.2 and test 2 display minimal fluctuation, whereas other tests exhibit pronounced variations. Notably, high friction occurs when the pitch angles are small, and conversely, low friction is observed when the pitch angles are larger.

The height fluctuation remains similar across all sliding speeds, despite changes in the average height value. As depicted in Fig. 8, the figure illustrates the height variation of different tests within one revolution at a sliding speed of 0.25 m/s. All tests exhibit a shared pattern of height fluctuation with three distinct peaks, aligning with the observed friction variation during rotation. Comparing Figs. 7 and 8, it could be observed that the low pitch angle are more likely to occurs on the "uphill" process (0–60°, 120°–180° and 240°–300°), where the pin is moving downwards away from the disc. It is noteworthy that the height variation is relatively small, measuring less than 10 μm for all tests, while the sliding radius is 30 mm, corresponding to a 188 mm sliding distance per rotation.

3.2. Simulation results

In order to explore the origin behind the experimental behaviour, numerical analysis was carried out for the given operating conditions. In Sim 1 the simulation was conducted using the roughness patch given in our previous study [21]. Fig. 9 presents the simulation results of the Stribeck curve with different experimental pin topographies. High consistence was observed for the pins in test 1, while curved pin in test 2 exhibit much higher friction.

The simulations in Sim 2 were carried out using the test speed and measured pin inclination, with parameters calibrated based on the test results of test 2. As depicted in Fig. 10, the CoF contour is presented concerning pitch angle and sliding speed for the averaged pin geometry in test 1. The results indicate that friction is influenced by both sliding speed and disc inclination. Even with a stable sliding speed, minor changes in disc inclination can markedly impact the friction coefficient. High friction levels were observed at low sliding speeds and low pitch angles. Conversely, low friction levels could be achieved, even at very low sliding speeds, when a converging inclination gap was established. Notably, at a converging inclination gap of 0.01° pitch angle, hydrodynamic friction was attained across the entire speed range. As the pitch angle decreased, friction increased, with the CoF rising from 0.014 to 0.068 for pitch angles decreasing from 0 to −0.01°, respectively.

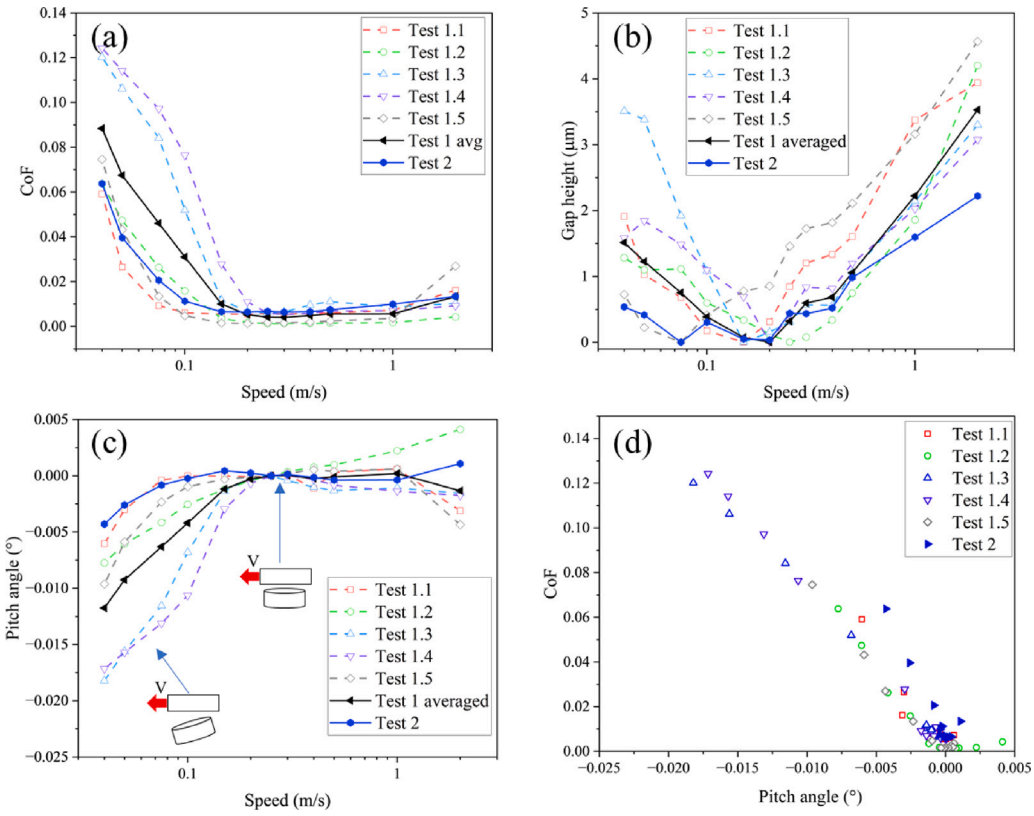

Fig. 5. Average (a) friction coefficient, (b) gap height and (c) pitch angle plotted against the sliding speed. (d) Average friction coefficient plotted against the relative pitch angle.

In Fig. 11, the pressure distribution at a sliding speed of 0.04 m/s is presented for pitch angles of 0.01°, 0°, and −0.01°, respectively. For the converging inclination gap of 0.01° pitch angle, elevated hydrodynamic pressure is observed across the entire surface (Fig. 11a). This results in the establishment of a higher gap height, leading to lower boundary friction and consequently, reduced overall friction. Conversely, in the case of a diverging gap at −0.01° (Fig. 11c), high hydrodynamic pressure is concentrated near the leading edge of the pin, accompanied by cavitation in the diverging area. This causes an increase in asperity contact pressure, resulting in elevated friction. The percentage of pressure shared by hydrodynamic and contact lift could be calculated based on the stress distribution. The ratio of contact load to the total load is noteworthy, with values of 0.4%, 6.6%, and 33.9% for pitch angles of 0.01°, 0°, and −0.01°, respectively. The hydrodynamic pressure change and their effect to friction form 0.1° to 0.1° is shown in Fig. S2 in the supporting information. This emphasizes the significant impact of pitch angle on the distribution of boundary pressures and, consequently, on the frictional behaviour within the tribological system.

Based on the simulation model, the CoF could be calculated according to the tested pitch angle. Fig. 12a gives the simulated average friction based on the test speed and measured pitch angle. Comparing to the test results (Fig. 5a), although there is difference in the absolute value, the simulation agrees with the experimental results in the trend. High friction appeared for the high inclination test 1.3 and 1.4. Fig. 12b shows the simulated friction variation within one revolution at 0.04 m/s. Comparing to Fig. 7a, the simulation explained well the friction behaviour in a rotation.

4. Discussions

4.1. Origins of test unrepeatability

Unrepeatability can arise due to various factors, including experimental setup variations, environmental conditions, measurement inaccuracies, or inherent variability in the system being studied. For the pin-on-disc tribological test in this study, among the various factors are pin macrogeometry and surface roughness.

As depicted in Fig. 2, the macrogeometry within test 1 exhibits a high degree of similarity among its components. It is challenging to attribute the notable frictional disparities observed to such minor differences in surface profiles alone. To further examine the factor, the curved pin in test 2 was investigated. In contrast to the pins utilized in test 1, the curved pin in test 2 featured a significantly smaller contact zone, while still large enough for a flat contact. Anticipating higher friction from both boundary and hydrodynamic perspectives in test 2, the results revealed, unexpectedly, that in some cases, pins from test 1 exhibited higher friction levels (Fig. 5a). The simulation results also suggested macrogeometry may not be the dominant factor, demonstrating the model's robustness to the surface profiles in test 1 (Fig. 9). This robustness implies that deviations observed in test 1 are unlikely to be solely attributed to variations in macroscopic geometry, prompting further investigation into the other factors influencing the observed tribological behaviours.

Surface roughness also plays a crucial role in friction. The model is sensitive to the roughness patches, as the roughness is directly related to the oil film thickness, which is a critical factor in generating hydrodynamic lift. However, attributing the differences observed in experiments solely to roughness may be insufficient for several reasons. Firstly, roughness examinations reveal minimal disparities in roughness measurements between test samples. It is unlikely that such slight differences in roughness could adequately compensate for the influence of macrogeometry variations observed between test 1 and test 2. Secondly, the differences in roughness could not explain the height waviness related CoF variation for the same pin and disc within one revolution. The intricate interplay between height waviness and friction suggests that factors beyond roughness contribute significantly to the observed differences in experimental outcomes.

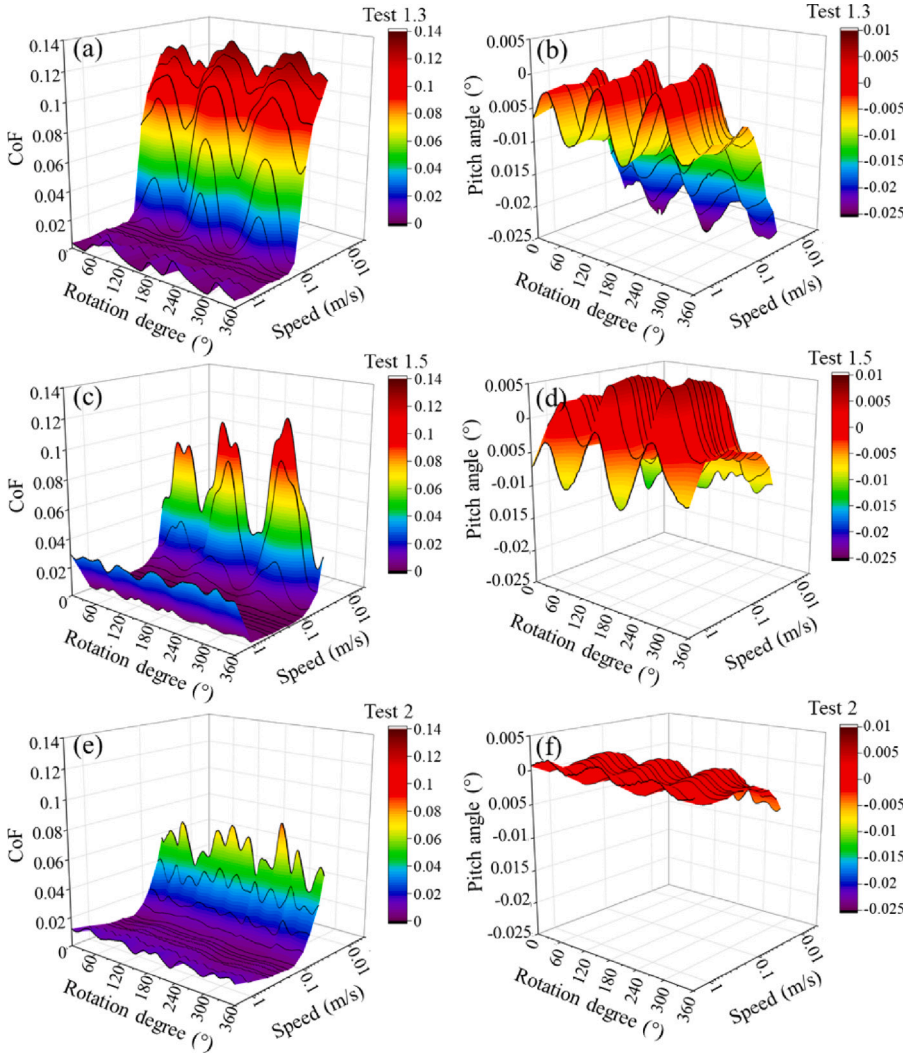

Fig. 6. CoF (a, c, e) and relative pitch angle (b, d, f) plotted against rotation angle and sliding speed. (a, b) test 1.3, (c, d) test 1.5 and (e, f) test 2. The relative pitch angle was plotted with average value at 0.25 mm/s as reference.

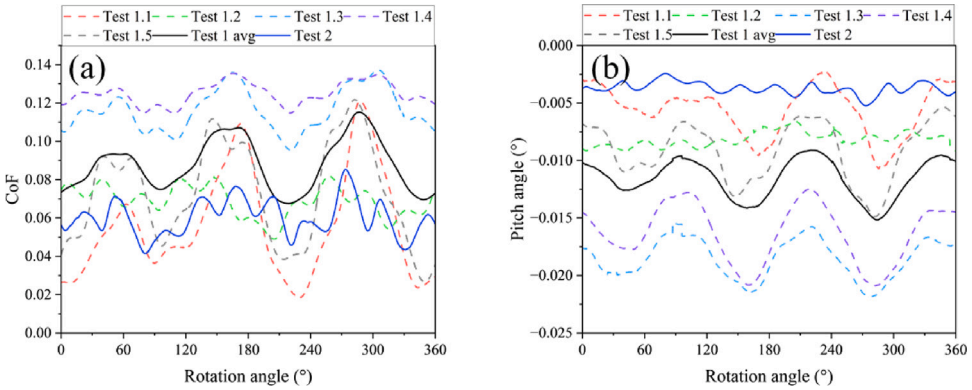

Fig. 7. CoF (a) and relative pitch angle (b) at 0.04 m/s plotted against rotation angle. The relative pitch angle was plotted with inclination height variation at 0.25 mm/s as reference.

Excluding macrogeometry and roughness, a prominent factor influencing frictional behaviour appears to be pin inclination. The variation in pin inclination results in the formation of converging or diverging gaps between the pin and the disc, potentially exerting a significant impact on friction. In the conducted tests, the inclination variations during sliding were successfully recorded. Notably, a distinct quasi-linear cor-

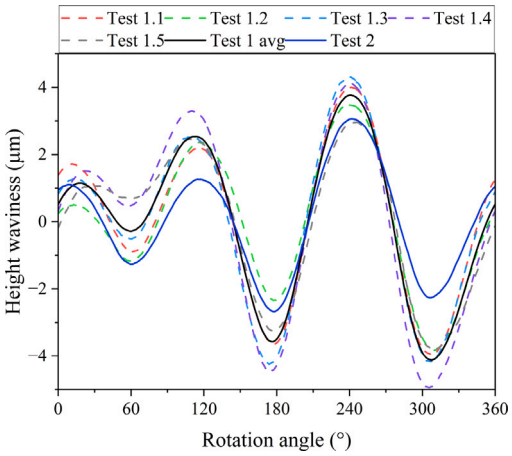

Fig. 8. Height waviness at 0.04 m/s plotted against rotation angle.

relation was evident in Fig. 5d between CoF and pin inclination. The observed correlation is rationalized by the fact that pin inclination is an outcome of force balance. Therefore, the robust correlation between pitch angle and friction is expected. The pivotal question arises: could the altered inclination, in turn, influence friction and contribute to the observed low repeatability in the experiments?

The most effective approach would be to conduct tests with fixed pin inclinations. However, due to the inherent challenges in controlling the very small pitch angle (0.01°) and the non-perfect flatness of the disc, achieving this control is not straightforward. As a potential solution, we introduced the curved pin 2 into the experimental setup. Theoretically, the inclination of a spherical surface would not lead to changes in the film profile, resulting in stable friction during sliding. The experimental results corroborated this assumption, demonstrating significantly lower friction fluctuation than anticipated (Fig. 7a). Further support for this notion was evident in our numerical studies. The numerical results distinctly showcased the influence of pitch angle on friction (Fig. 10), providing a comprehensive explanation for the observed friction disparities in the experiments.

4.2. Limitations in the simulation

In the simulation for the influence of pin inclinations, the model was initially calibrated using the curved pin in test 2. Subsequently, numerical analyses were performed utilizing the test speed and measured pin inclination data from test 1. The simulation results effectively elucidated the distinctions observed in test 1 and the fluctuations in friction during sliding. Nonetheless, some discrepancies persist due to necessary simplifications and gaps in our knowledge about the test conditions.

Firstly, in the simulation, the influence of pin inclination was primarily analysed from a hydrodynamic perspective. The boundary friction coefficient in the model was set as a constant (0.192) based on the theoretical derivation by Bowden and Tabor [22]. However, adhering to the principles of boundary lubrication, friction should be correlated with boundary film thickness and durability. It is conceivable that the boundary film may be prone to failure under high contact stress, resulting in an elevated boundary friction coefficient.

Secondly, the model is founded on the homogenized method, wherein the hydrodynamic effect is governed for a full film in the mean gap height with adjustments made by homogenization factors. In reality, under sufficiently high loads, the contact region may impede oil flow, undermining the hydrodynamic component in mixed lubrication. This scenario could lead to elevated friction in cases of diverging pin inclination.

Meanwhile, the cavitation treatment in a simulation is rather complex and challenging [23,24]. Different models lead to different behaviour in hydrodynamic pressure distribution, especially in the divergent zone. When negative pitch angles were formed between pin and disc, a very large divergent zone was generate. This might affect the reliability of the numerical results.

4.3. Formation of pin inclination

The pin inclination results from a force balance mechanism, as illustrated in Fig. 13. Fig. 13a details the force balance for the hydrodynamic component. In the case of full film sliding where friction force is minimal, the pin primarily experiences the load (N). If the load is applied near the leading or rear edge, a torque is generated, pushing the pin back to its equilibrium position. Consequently, the pitch angles remain relatively stable at high speeds (Fig. 5c). Concerning the boundary component (Fig. 13b), the pin encounters both a load (N) and a friction force (F), with the corresponding reaction force generated from the supporting bearing. If only centripetal force acts on the bearing, it would create a counter-clockwise torque (T), contributing to the generation of a converging inclination gap. However, the friction force between the upper and lower bearing will cause reaction force against the sliding direction. Therefore, the reaction force becomes non-centripetal, inducing a clockwise torque, leading to a diverging inclination gap (Fig. 13c). This divergence will in turn result in increased boundary friction force. Consequently, even a minor disturbance can escalate into a significant difference in friction.

Fig. 14 shows the typical force balance state for the pin during sliding. Ideally, if the full film lubrication were achieved, a converging gap would be formed. The inclination pitch angle would reach an equilibrium state based on the hydrodynamic pressure distribution. Fig. 14a shows the 2D schematic pressure distribution profile and equivalent acting point of force. With the speed decreasing, the two surfaces come into contact. As the contact friction is much higher than the hydrodynamic friction, a clockwise torque will be applied on the pin, resulting in the rotation of the pin. Finally, the pin would reach a certain angle such that the friction and loading forces reach the equilibrium state (Fig. 14b). In practice, the equilibrium state for pin inclination is intricate, and similar analyses can be found in the context of tilting pad bearings [20,25]. However, due to variations in setups for pin-on-disc tests, devising a comprehensive solution is challenging.

The sliding interaction between the pin and the disc constitutes a dynamic process characterized by changes in inclination. This process could be influenced by factors such as the height waviness of the disc, the inlet/outlet profile of the pins, local roughness of the disc, friction around the pivot of pin holder or system vibrations. In certain instances, if the factors are favourable, the inclination remains stable, resulting in a consistent friction force (as observed in test 1.2 in Fig. 7). Conversely, in other cases, the inclination undergoes continuous build-up and failure, leading to pronounced fluctuations in friction. As shown in Fig. 15, the inclination may be affected by the height waviness along the sliding path. The height waviness of disc surface will form a certain angle variation of the surface. During sliding, the pin will rotate around the self-aligning pivot when the path slope is changed. In some cases the same inclination state will persist for the whole rotation (Fig. 15a), leading to stable friction. However, in practice, there are instances where the rotation may not accurately correspond to the height variation, leading to a change in the pitch angle (Fig. 15b). When the pin transitions from a downhill to an uphill trajectory, a negative pitch angle is likely to manifest, resulting in elevated friction. Conversely, in the opposite scenario where the pin shifts from an uphill to a downhill trajectory, a converging gap emerges, leading to reduced friction. This state of inclination may persist throughout the uphill or downhill process. This is why the high friction was more likely to occur in the uphill stage.

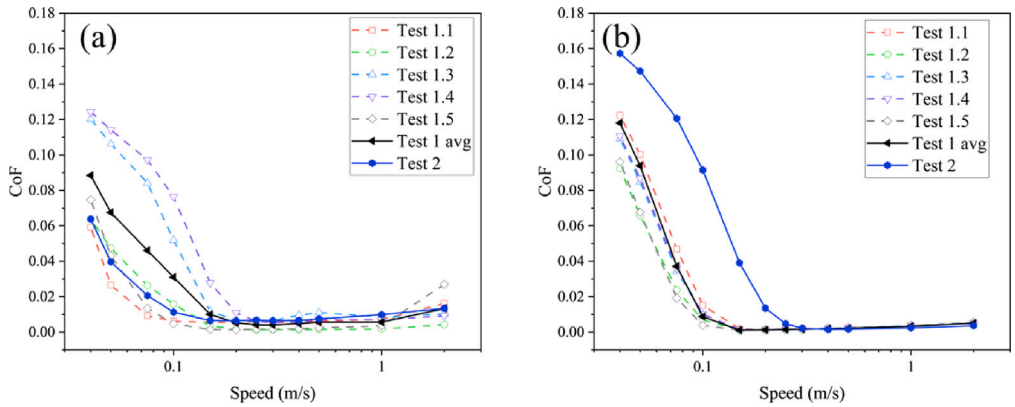

Fig. 9. Friction coefficient plotted against the sliding speed. (a) Experiment results. (b) Simulation results (Sim 1).

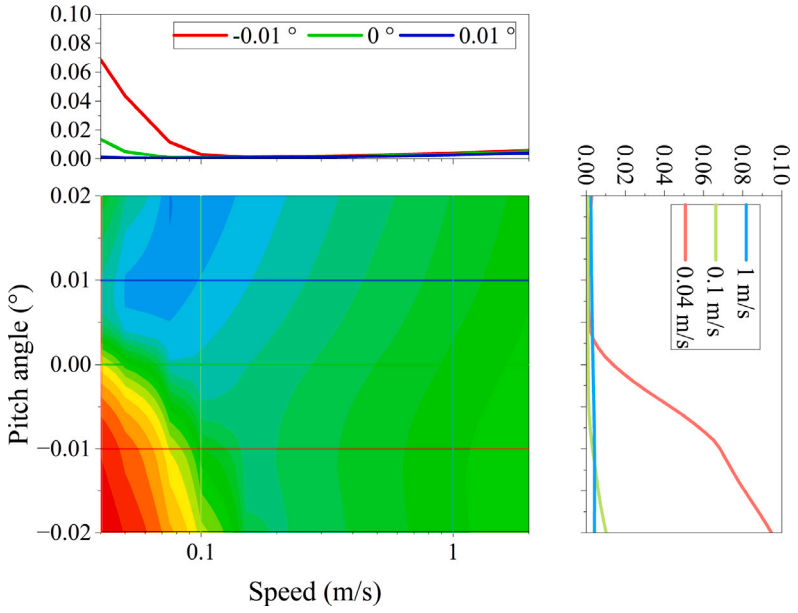

Fig. 10. Simulated CoF plotted against sliding speed and pitch angle for averaged pin geometry (Sim 2).

4.4. Implications for test reliability

In the experiment, variation of pin inclination was observed during sliding of a self-aligning pin. Analysis suggests the inclined pin will in turn affect the friction between pin and disc. However, the formation of the inclination seemed quite sensitive to the operating conditions and the mechanism behind it remains to be investigated. These findings raise substantial concerns about the reliability of the pin-on-disc tribotest. It suggests that the measured friction may be more influenced by the equilibrium of inclination rather than the intrinsic material or surface properties. This concern becomes particularly significant for tests involving modifications to sample surface topography, such as changes in roughness or surface texturing. Some studies suggested surface texturing may affect the equilibrium state of tilting pad bearing [26,27], which may also apply to the pin-on-disc setups.

Although the inclination changes were investigated in our tribometer, this factor remains a potential variable in all pin-on-disc tests utilizing self-aligning pins. The test error may vary under different operation conditions, including load, surface roughness, disc flatness or other factors. Theoretically, a consistent inherent friction coefficient should result in a fixed inclination state. If high test repeatability was observed, it would facilitate meaningful comparisons of material impacts. However, it is noteworthy that the absolute friction value might be re-scaled due to the different pin inclination state.

One approach to address this challenge is using a fixed pin, though this introduces complexities in setting the initial state. In some instances, tests could be run until the surface naturally aligns due to wear. However, this method risks destroying the surface topography. Another option involves employing spherical pins. Using a large radius is vital to prevent the test from evolving into a ball-on-disc configuration. However, this approach poses challenges in sample preparation and is only suitable for low-wear scenarios. Once wear occurs, the flattened surface becomes sensitive to pin inclination, limiting the applicability of this method.

An optimal approach might be to implement test protocols designed to eliminate the influence of the inclination factor. As an option, a flat contact ring-on-disc setup [28,29] for rotational tests, or using two small samples with a long span [30] for reciprocating tests, might be effective in minimizing this test error (Fig. 16).

5. Conclusions

In this investigation, we examined the impact of pin inclination on frictional behaviours in pin-on-disc tests through a combination of experimental and numerical methods. In-situ inclination was measured during the pin-on-disc rotational test, and a HMEHL-FBNS model was employed for numerical evaluation. The results revealed that even a minor misalignment of the pin, approximately 0.01°, had a significant

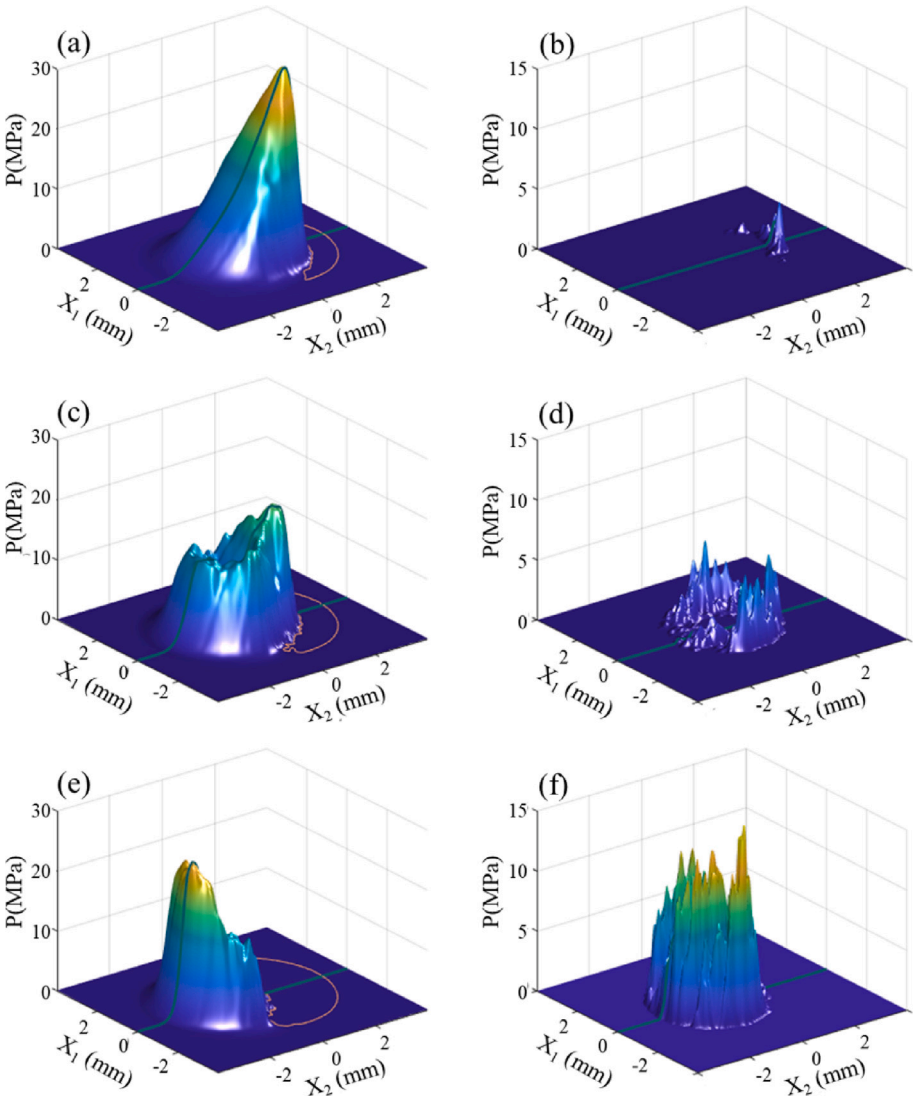

Fig. 11. Pressure distribution contour for the averaged pin profile in Sim 2 with (a, b) 0.01, (c, d) 0 and (e, f) −0.01° pitch angle. (a, c, e) Hydrodynamic pressure. (b, d, f) Contact pressure.

impact on lubrication state and friction. This observation provides a plausible explanation for variations between different samples and the observed fluctuations within the same sample.

Our study raises concerns about the reliability of the pin-on-disc test, suggesting that lower friction may be attributed more to a favourable equilibrium inclination state rather than intrinsic material or surface properties. Regrettably, at present, we do not identify any feasible solutions to overcome this challenge. Further exploration and advancements in testing methodologies may be necessary to address and mitigate the influence of pin inclination on test outcomes.

CRediT authorship contribution statement

Hongzhi Yue: Writing – review & editing, Writing – original draft, Validation, Software, Project administration, Methodology, Investigation, Formal analysis, Data curation, Conceptualization. **Johannes Schneider:** Writing – review & editing, Supervision, Project administration, Conceptualization. **Bettina Frohnapfel:** Writing – review & editing, Supervision, Resources, Project administration, Funding acquisition, Conceptualization. **Peter Gumbsch:** Writing – review & editing, Supervision, Resources, Project administration, Funding acquisition, Conceptualization.

Declaration of competing interest

The authors declare the following financial interests/personal relationships which may be considered as potential competing interests: The authors report financial support was provided by Deutsche Forschungsgemeinschaft (DFG) Project and KIT-Publication Fund of the Karlsruhe Institute of Technology. If there are other authors, they declare that they have no known competing financial interests or personal relationships that could have appeared to influence the work reported in this paper.

Data availability

Data will be made available on request.

Acknowledgement

The authors express their gratitude for the invaluable assistance provided by Dr. Gerda Vaitkunaite and Dr. Erik Hansen in guidance for conducting experiments and simulations. This research was funded by Deutsche Forschungsgemeinschaft (DFG) Project Number 438122912. We acknowledge support by the KIT-Publication Fund of the Karlsruhe Institute of Technology.

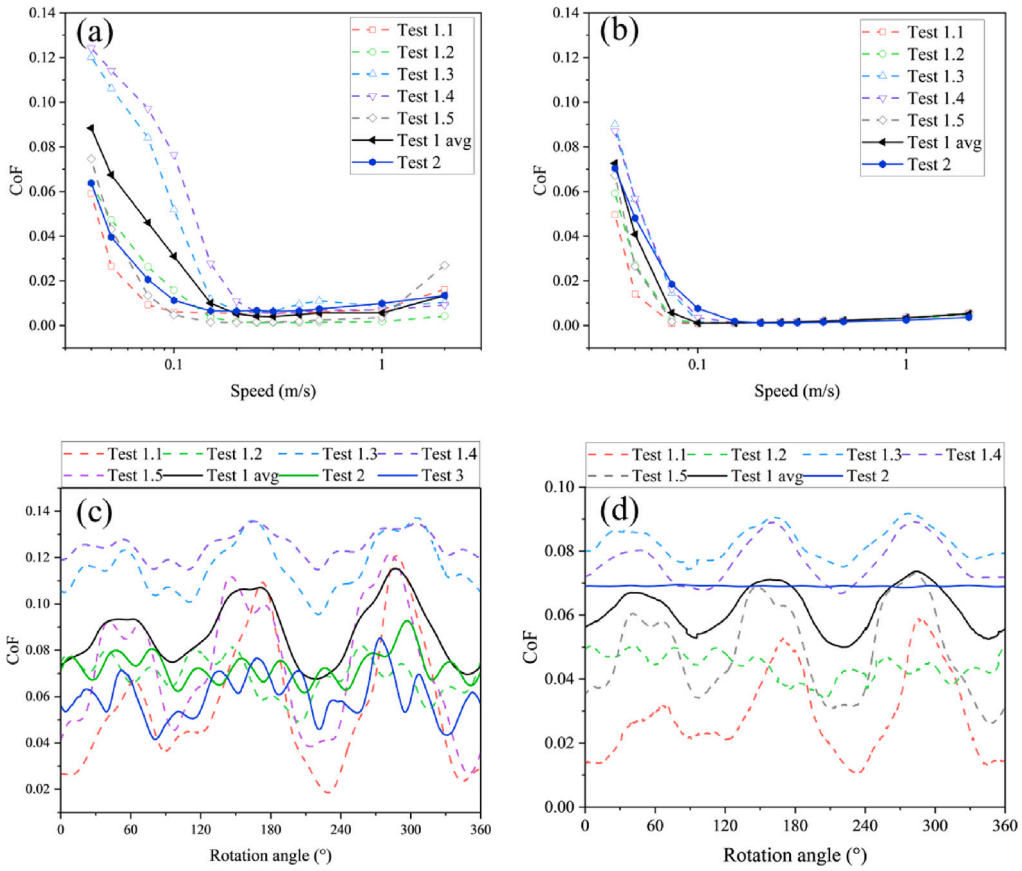

Fig. 12. Averaged CoF plotted against sliding speed (a, b) and CoF variation at 0.04 m/s plotted against rotation angle(c, d). (a, c) Experiment results. (b, d) Simulation results (Sim 2).

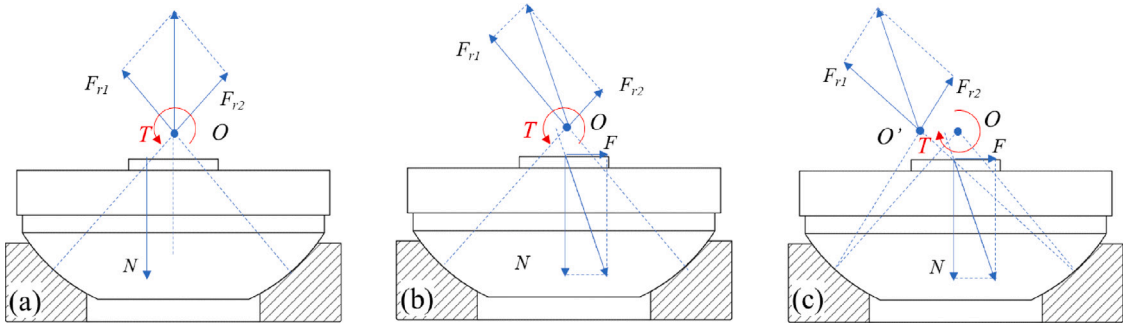

Fig. 13. Force diagram for a self-aligning pin. (a) Hydrodynamic component. (b) Contact component with centripetal reaction force. (c) Contact component with non-centripetal reaction force.

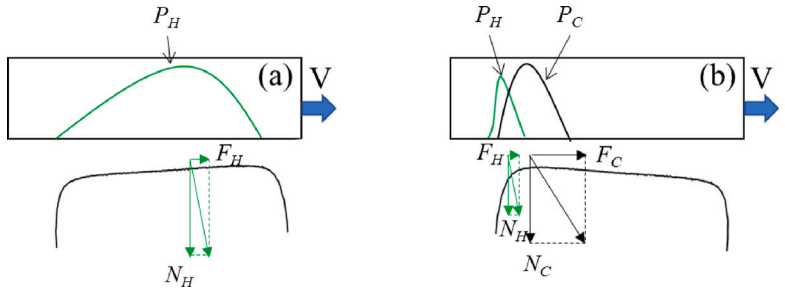

Fig. 14. Schematic representation of equilibrium state at (a) Hydrodynamic lubrication regime and (b) mixed lubrication regime. P_H: Hydrodynamic pressure; P_C: Contact pressure; N_H: Hydrodynamic load; F_H: Hydrodynamic friction; N_C: Contact load; F_C: Contact friction.

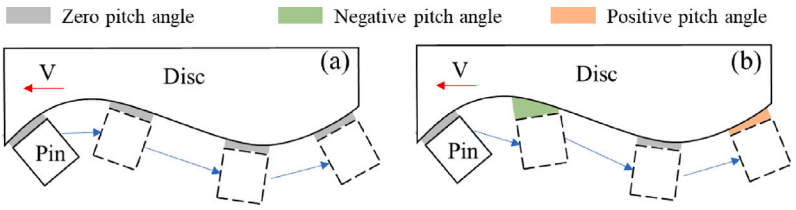

Fig. 15. Schematic representation of pin inclination generation due to disc height waviness. (a) Stable inclination. (b) Varied inclination.

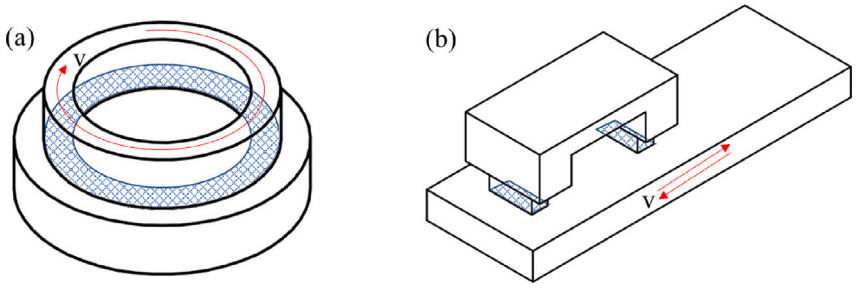

Fig. 16. Schematic representation of test setups to mitigate inclination effect. (a) Ring-on-disc test. (b) Long span pin-on-disc test.

Appendix A. Supplementary data

Supplementary material related to this article can be found online at https://doi.org/10.1016/j.triboint.2024.110083.

References

[1] Chang K, Soshi M. Optimization of planar honing process for surface finish of machine tool sliding guideways. J Manuf Sci Eng 2017;139(7):071015. http://dx.doi.org/10.1115/1.4036224.

[2] Altintas Y, Verl A, Brecher C, Uriarte L, Pritschow G. Machine tool feed drives. CIRP Ann 2011;60(2):779–96. http://dx.doi.org/10.1016/j.cirp.2011.05.010.

[3] Verma PC, Menapace L, Bonfanti A, Ciudin R, Gialanella S, Straffelini G. Braking pad-disc system: Wear mechanisms and formation of wear fragments. Wear 2015;322:251–8. http://dx.doi.org/10.1016/j.wear.2014.11.019.

[4] Eriksson M, Lord J, Jacobson S. Wear and contact conditions of brake pads: dynamical in situ studies of pad on glass. Wear 2001;249(3–4):272–8. http://dx.doi.org/10.1016/S0043-1648(01)00573-7.

[5] Mayer E. Mechanical seals. Butterworth-Heinemann; 2013.

[6] Persson BNJ, Albohr O, Tartaglino U, Volokitin AI, Tosatti E. On the nature of surface roughness with application to contact mechanics, sealing, rubber friction and adhesion. J Phys: Condensed Matter 2004;17(1):R1. http://dx.doi.org/10.1088/0953-8984/17/1/R01.

[7] Di Puccio F, Mattei L. Biotribology of artificial hip joints. World J Orthop 2015;6(1):77. http://dx.doi.org/10.5312/wjo.v6.i1.77.

[8] Wang QJ. Conformal-contact elements and systems. In: Wang QJ, Chung Y-W, editors. Encyclopedia of tribology. Boston, MA: Springer US; 2013, p. 434–40.

[9] ISO 7148-1:1999. Plain bearings—Testing of the tribological behaviour of bearing materials—Part 1: Testing of bearing metals. Standard, Geneva, CH: International Organization for Standardization; 2001.

[10] ISO 7148-2:1999. Plain bearings—Testing of the tribological behaviour of bearing materials—Part 2: Testing of polymer-based bearing materials. Standard, Geneva, CH: International Organization for Standardization; 2001.

[11] Braun D, Greiner C, Schneider J, Gumbsch P. Efficiency of laser surface texturing in the reduction of friction under mixed lubrication. Tribol Int 2014;77:142–7. http://dx.doi.org/10.1016/j.triboint.2014.04.012.

[12] Suh AY, Patel JJ, Polycarpou AA, Conry TF. Scuffing of cast iron and Al390-T6 materials used in compressor applications. Wear 2006;260(7):735–44. http://dx.doi.org/10.1016/j.wear.2005.04.013.

[13] Wos S, Koszela W, Pawlus P. Determination of oil demand for textured surfaces under conformal contact conditions. Tribol Int 2016;93:602–13. http://dx.doi.org/10.1016/j.triboint.2015.05.016.

[14] Godfrey D. Friction oscillations with a pin-on-disc tribometer. Tribol Int 1995;28(2):119–26. http://dx.doi.org/10.1016/0301-679X(95)92701-6.

[15] Hsiao E, Kim SH. Analyzing periodic signals in rotating pin-on-disc tribotest measurements using discrete Fourier transform algorithm. Tribol Lett 2009;35(2):141–7. http://dx.doi.org/10.1007/s11249-009-9462-2.

[16] Li Y, Garabedian N, Schneider J, Greiner C. Waviness affects friction and abrasive wear. Tribol Lett 2023;71(2):64. http://dx.doi.org/10.1007/s11249-023-01736-1.

[17] Prost J, Boidi G, Lebersorger T, Varga M, Vorlaufer G. Comprehensive review of tribometer dynamics-Cycle-based data analysis and visualization. Friction 2022;1–15. http://dx.doi.org/10.1007/s40544-021-0534-0.

[18] Bhushan B, Ko PL. Introduction to tribology. Appl Mech Rev 2003;56(1):B6–7.

[19] Liu Y, Xie X, Wang B, Wang R, Yan G, Jia Q, Yuan X. Analysis of transient and static lubrication performance of tilting pad thrust bearing considering pivot deformation. Tribol Int 2023;190:109066. http://dx.doi.org/10.1016/j.triboint.2023.109066.

[20] Dimond T, Younan A, Allaire P. A review of tilting pad bearing theory. Int J Rotating Mach 2011;2011:1–23. http://dx.doi.org/10.1155/2011/908469.

[21] Hansen E, Vaitkunaite G, Schneider J, Gumbsch P, Frohnapfel B. Establishment and calibration of a digital twin to replicate the friction behaviour of a pin-on-disk tribometer. Lubricants 2023;11(2):75. http://dx.doi.org/10.3390/lubricants11020075.

[22] Bowden FP, Tabor D. The friction and lubrication of solids, Vol. 1, Oxford University Press; 2001.

[23] Braun MJ, Hannon WM. Cavitation formation and modelling for fluid film bearings: A review. Proc Inst Mech Eng J: J Eng Tribol 2010;224(9):839–63. http://dx.doi.org/10.1243/13506501JET772.

[24] Çam MY, Giacopini M, Dini D, Biancofiore L. A numerical algorithm to model wall slip and cavitation in two-dimensional hydrodynamically lubricated contacts. Tribol Int 2023;184:108444. http://dx.doi.org/10.1016/j.triboint.2023.108444.

[25] Zhang C, Yu W, Zhang L. Dynamic characteristics of tilting-pad coupled-bearing-rotor systems considering mixed lubrication and pad wear. Tribol Int 2024;192:109287. http://dx.doi.org/10.1016/j.triboint.2024.109287.

[26] Yagi K, Sugimura J. Performance of balancing wedge action in textured hydrodynamic pad bearings. J Tribol 2017;139(1):011704. http://dx.doi.org/10.1115/1.4033128.

[27] Gropper D, Harvey TJ, Wang L. Numerical analysis and optimization of surface textures for a tilting pad thrust bearing. Tribol Int 2018;124:134–44. http://dx.doi.org/10.1115/1.4033128.

[28] Wang X, Kato K, Adachi K, Aizawa K. The effect of laser texturing of SiC surface on the critical load for the transition of water lubrication mode from hydrodynamic to mixed. Tribol Int 2001;34(10):703–11. http://dx.doi.org/10.1016/S0301-679X(01)00063-9.

[29] Schnell G, Müller T, Seitz H. Tribological effects of different scaled chevron-shaped microstructures on the Stribeck curve of parallel contacts under unidirectional friction. Tribol Int 2023;178:108099. http://dx.doi.org/10.1016/j.triboint.2022.108099.

[30] Ryk G, Kligerman Y, Etsion I. Experimental investigation of laser surface texturing for reciprocating automotive components. Tribol Trans 2002;45(4):444–9. http://dx.doi.org/10.1080/10402000208982572.